IAC-16-A6.2.11

Spacecraft design optimisation for demise and survivability

Mirko Trisolini[a]*, Hugh G. Lewis[a], Camilla Colombo[b]

[a] *Astronautics Research Group, University of Southampton, Southampton , SO17 1BJ, United Kingdom,* m.trisolini@soton.ac.uk, H.G.Lewis@soton.ac.uk
[b] *Department of Aerospace Science and Technology, Politecnico di Milano, Via La Masa 34, 20133, Milan, Italy,* camilla.colombo@polimi.it
* Corresponding Author

Abstract

Among the mitigation measures introduced to cope with the space debris issue there is the de-orbiting of decommissioned satellites. Guidelines for re-entering objects call for a ground casualty risk no higher than 10^{-4}. To comply with this requirement, satellites can be designed through a design-for-demise philosophy. Still, a spacecraft designed to demise through the atmosphere has to survive the debris populated space environment for many years. The demisability and the survivability of a satellite can both be influenced by a set of common design choices such as the material selection, the geometry definition, and the position of the components inside the spacecraft. Within this context, two models have been developed to analyse the demise and the survivability of satellites. Given the competing nature of the demisability and the survivability requirements, a multi-objective optimisation framework was developed, with the aim to identify trade-off solutions for the preliminary design of satellites. As the problem is nonlinear and involves the combination of continuous and discrete variables, classical derivative based approaches are unsuited and a genetic algorithm was selected instead. The genetic algorithm uses the developed demisability and survivability criteria as the fitness functions of the multi-objective algorithm. The paper presents a test case, which considers the preliminary optimisation of tanks in terms of material, geometry, location and number of tanks for a representative Earth observation mission. The configuration of the external structure of the spacecraft is fixed. Tanks were selected because they are sensitive to both design requirements: they represent critical components in the demise process and impact damage can cause the loss of the mission because of leaking and ruptures. The results present the possible trade off solutions, constituting the Pareto front obtained from the multi-objective optimisation.

Keywords: design-for-demise, survivability, multi-objective optimisation, tanks

Nomenclature

a	Semi-major axis
C	Speed of sound
CD	Drag coefficient
C_m	Heat capacity
E_0	Maximum allowed displacement from the nominal ground track at the equator
g_0	Gravitational acceleration at sea level
h	Altitude
h_f	Heat of fusion
Isp	Specific impulse
$K1$	Factor to account for the additional tank volume for the pressuring gas
$K2$	Factor to account for the separation between two tanks
l	Distance between two tanks
L	Side length of the spacecraft
m	Mass
N	Total number of spacecraft components
n_t	Number of tanks
Pp	Penetration probability
r	Radius
S	Cross-section of the spacecraft
s	Thickness
t_m	Mission duration
T_m	Melting temperature
V	Velocity
v	Volume
γ	Flight path angle
ε	Emissivity
λ	Longitude
ρ	Density
σ_y	Yield strength
σ_u	Ultimate tensile strength
φ	Latitude
χ	Heading angle
ω	Angular velocity

Subscripts

0	Nominal orbit
1	Start orbit for the Hohmann transfer
2	Final orbit of the Hohmann transfer
atm	Atmosphere
$decay$	Relative to decaying correction manoeuvres
$disp$	Relative to disposal manoeuvres

e	Earth
f	Fuel
fin	Final condition
in	Initial condition
inc	Relative to inclination change manoeuvres
inj	Relative to orbit injection errors
mat	Material
p	Propellant
s	Spacecraft
sec	Relative to secular variations of the orbital parameters
t	Tank
tot	Total

Acronyms

DAS	Debris Assessment Software
LMF	Liquid Mass Fraction
BLE	Ballistic Limit Equation
SRL	Schafer-Ryan-Lambert
NSGA	Non-dominated Sorting Genetic Algorithm
PNP	Probability of no-penetration

1 Introduction

In the past two decades, the attention on a more sustainable use of outer space has increased steadily. The major space-faring nations and international committees have proposed a series of debris mitigation measures [1, 2] to protect the space environment. Among these mitigation measures, the de-orbiting of spacecraft at the end of their operational life is recommended in order to reduce the risk of on-orbit collisions.

Re-entering spacecraft can pose a risk to people and property on the ground. Therefore, their casualty risk needs to be assessed as it needs to comply with the casualty limit of 10^{-4} if an uncontrolled re-entry strategy is to be adopted [3, 4]. A possible strategy to limit the ground casualty risk is to use a design for demise philosophy, where most (if not all) of the spacecraft will not survive the re-entry process. The implementation of design for demise strategies [5-7] may favour the selection of uncontrolled re-entry disposal options over controlled ones, leading to a simpler and cheaper alternative for the disposal of a satellite at the end of its operational life [6, 7]. However, a spacecraft designed for demise still has to survive the space environment for many years. As a large number of space debris and meteoroids populates the space around the Earth, a spacecraft can suffer impacts from these particles, which can be extremely dangerous, damaging the spacecraft or even causing the complete loss of the mission [8-10]. This means that the spacecraft design has also to comply with the requirements arising from the survivability against debris impacts. The demisability and survivability of a spacecraft are both influenced by a set of common design choices, such as the structural material, shape, dimension and position inside the spacecraft. It is important to consider such design choices and how they influence the mission's survivability and demisability from the early stages of the mission design process [7]. Taking into consideration these requirements at a later stage of the mission may cause an inadequate integration of these design solutions, leading to a delayed deployment of the mission and to an increased cost of the project. On the other hand, an early consideration of such requirements can favour cheaper options such as the uncontrolled re-entry of the satellite, whilst maintaining the necessary survivability and, thus, the mission reliability.

With these considerations, two models have been developed [11] to assess the demisability and the survivability of simplified mission designs as a function of different design parameters. Two criteria are presented to evaluate the degree of demisability and survivability of a spacecraft configuration. Such an analysis can be carried out on many different kinds of missions, provided that they can be disposed through atmospheric re-entry and they experience impacts from debris particles during their operational life. These characteristics are common to a variety of missions; however, it was decided to focus the current analysis on Earth observation and remote sensing missions. Many of these missions exploit sun-synchronous orbits due to their favourable characteristics, where a spacecraft passes over any given point of the Earth's surface at the same local solar time. Because of their appealing features, sun-synchronous orbits have high commercial value. Alongside their value from the commercial standpoint, they are also interesting for a combined survivability and demisability analysis. Sun-synchronous missions can in fact be disposed through atmospheric re-entry. They are also subject to very high debris fluxes [12] making them a perfect candidate for the purpose of this study.

Given the competing nature of the demisability and survivability requirements, a multi-objective optimisation framework was developed, with the aim to find trade-off solutions for the preliminary design of satellites. As the problem is nonlinear and involves the combination of continuous and discrete variables, classical derivative based approaches are unsuited and a genetic algorithm was selected instead. The genetic algorithm uses the previously described demise and survivability criteria as the fitness functions of the multi-objective algorithm.

The paper presents a test case, which considers the preliminary optimisation of tanks in terms of material, geometry, location and number of tanks for representative sun-synchronous missions. The configuration of the external structure of the spacecraft was fixed. Tanks were selected because they are

interesting for both the survivability and the demisability. They represent critical components in the demisability analysis as they usually survive the atmospheric re-entry. They are also components that need particular protection from the impact against space debris because the impact with debris particles can cause leaking or ruptures, which can compromise the mission success. Different configurations were analysed as a function of the characteristics of the tank assembly and of the mission itself, such as the mission duration and the mass class of the spacecraft. The results are presented in the form of Pareto fronts, which represent the different possible trade-off solutions.

2 Demisability and Survivability Models

In order to carry out a combined demisability and survivability analysis of a spacecraft configuration it was necessary to develop two models [11, 13]. One model allows the analysis of the atmospheric re-entry of a simplified spacecraft configuration in order to evaluate its demisability. The other model carries out a debris impact analysis and returns the penetration probability of the satellite as a measure of its survivability. As these two models need to be implemented into an optimisation framework, much effort was made to maintain a comparable level of detail and computational time between them.

2.1 Demisability model

The developed demisability model consists of an object-oriented code [14-16]. The main features of this type of code is the fast simulation of the re-entry of a spacecraft that is schematised using primitive shapes such as spheres, cubes, cylinders, and flat plates. These primitive shapes are used as a simplified representation of both the main spacecraft structure and internal components. The different parts of the spacecraft are defined in a hierarchical scheme with the main structure being the parent object and the internal components being the child objects that are contained inside the parent structure. For the simplified nature of the simulation carried out in object-oriented codes, the internal components do not experience any heat load until the main break-up event occurs. In the current model the break-up altitude is user-defined and is set to a default value of 78 km, which is the standard value used in most destructive re-entry software [17]. After the break-up occurs the child objects are separated from the main structure and their re-entry is simulated separately. The trajectory of the spacecraft is simulated with three degree-of-freedom ballistic dynamics. The computation of the attitude motion of the spacecraft is neglected and assumed to be random tumbling. Motion and shape averaged drag coefficients [18-20] are used for the aerodynamics of the spacecraft. The thermal load is computed using the Detra-Kemp-Riddel [20, 21] correlation and a set of motion and shape averaged shape factors [17, 18, 22, 23]. Standard models for the Earth's atmosphere and the gravitational field are used. Respectively, the 1976 U.S Standard Atmosphere [24], and the zonal harmonic gravity model up to degree four [25] are adopted. The material database used is the one available in the NASA Debris Assessment Software (DAS) [15].

The demise of components, i.e. the mass loss during the re-entry, is analysed using a lumped mass model where the temperature of the components remains uniform over its entire volume. After the melting temperature is reached, the object starts to melt at a rate that is proportional to the heat load and the heat of fusion of the material.

2.2 Survivability model

The survivability model analyses the spacecraft configuration against the impact from untrackable space debris and meteoroids. For this procedure, the spacecraft was schematised with a panelised representation. To each panel is assigned a material and its geometrical properties, as well as the type of shielding. The survivability model uses the same geometrical shapes of the demisability model in order to keep the two models comparable. Alongside the geometrical representation of the satellite, the characteristics of the space environment need to be known. This is achieved using the European Space Agency (ESA) software MASTER-2009 [26], which provides debris flux predictions for user defined target orbits. The 2D and 3D debris fluxes obtained from MASTER-2009 are used in conjunction with the geometrical characteristics of the spacecraft and the ballistic limit equations (BLE) to compute the penetration probability on each panel in which the structure is schematised using Poisson statistics [10, 27-29]. A more complete description of the procedure can be found in [11, 13].

A distinction needs to be made between the external structure of the spacecraft and the internal components. For the external structure, there is a direct impact with the space debris leading to the direct application of the procedure outlined before. On the other hand, when considering internal components, the debris clouds that develop inside the spacecraft after the impact need to be considered [8-10, 27]. These clouds can in fact hit and damage internal components. To consider how the impacts on the outer structure propagate into the inner components, two tools have been used: the Schafer-Ryan-Lambert ballistic limit equation (SRL-BLE) [10, 27], which can take into account impacts on multi-walled structures (up to three layers), and the concept of *vulnerable areas* [9]. The vulnerable area consists of an adjusted projection of an inner component onto the outer spacecraft structure. This area represents the

portion of the external structure that, if impacted by a particle, could also lead to the impact of the inner component to which the relevant vulnerable area is associated. The SRL-BLE subsequently allows the direct calculation of the critical diameter associated with the inner components walls. In addition to the computation of the vulnerable areas and the critical diameters for the individual components, it is also necessary to consider the position of the components, and their mutual interaction inside the spacecraft. In fact, the position of the components inside the spacecraft produces mutual shielding of the components, reducing their vulnerability. The final step in the analysis is the computation of the vulnerability of each component inside the spacecraft and its external structure.

3 Sun-synchronous Missions

As mentioned, for the presented analysis we are considering the optimisation of tank configurations of Earth observation and remote sensing missions [30, 31]. These kinds of missions frequently exploit sun-synchronous orbits and that is the reason why the current work focuses on these orbits. A sun-synchronous orbit is a Low Earth Orbit (LEO) that combines altitude and inclination in order for the satellite to pass over any given point of the Earth's surface at the same local solar time, granting the satellite a view of the Earth's surface at nearly the same illumination angle and sunlight input. To estimate the size of the tank assembly it is necessary to compute the amount of propellant needed for the mission through a delta-V budget. As sun-synchronous orbits are influenced by atmospheric drag and by the non-uniformity of the Earth's gravitational field, they require regular orbit correction manoeuvres. They also need, as for most spacecraft, additional manoeuvres to correct orbit injection errors and to perform disposal manoeuvres. The computation of the different contributions to the delta-V budget is described in the following paragraph.

3.1 Delta-V budget

To estimate the tankage volume it is necessary to compute the amount of propellant needed by the spacecraft as a function of the mission characteristics. The three main elements that contribute to the ΔV budget for the required mission lifetime are the orbit maintenance, the launch injection errors, and the disposal manoeuvres.

Orbit maintenance manoeuvres are used to maintain the sun-synchronism of the orbit and to control the ground track with a given accuracy. To do so, the orbital height and inclination need to be maintained within admissible ranges. In LEO, atmospheric drag results in orbital decay, causing the semi-major axis and the orbit period to decrease. The reduction in the semi-major axis δa and in the orbital period $\delta\tau$ for one orbit can be computed as

$$\delta a = -2\pi\rho_{atm}\frac{SC_D}{m_s}a_0^{\,2} \tag{1}$$

$$\delta\tau = \frac{3\pi}{V_s}\delta a \tag{2}$$

where ρ_{atm} is the atmospheric density, S is the average cross section of the satellite, C_D is the drag coefficient, m_s is the mass of the satellite, a_0 is the nominal orbit semi-major axis, and V_s is the orbital velocity of the spacecraft. The changes in the orbital height and period lead to changes in the ground track. Such variations can be controlled by imposing a tolerance on the nominal ground track. When the spacecraft's ground track reaches the prescribed tolerance, a correction manoeuvre needs to be executed. To do so, the time difference from the nominal time at the equator passage Δt_0 needs to be computed:

$$\Delta t_0 = \frac{\Delta\lambda}{\omega_e} \tag{3}$$

where ω_e is the angular speed of the Earth and $\Delta\lambda$ is the longitude displacement at equator passage and can be expressed as:

$$\Delta\lambda = \frac{2E_0}{r_e} \tag{4}$$

r_e is the radius of the Earth, and E_0 is the imposed tolerance on the displacement from the nominal orbit ground track at the equator (equal to 0.7 km for this study). Using Eqs. (3) and (4) It is possible to compute the number of orbits after which the equator crossing displacement reaches the prescribed limit as follows:

$$k = \sqrt{\frac{2\Delta t_0}{\delta\tau}} \tag{5}$$

To control the ground track, the manoeuvre has to be executed every $2k$ orbits, leading to a variation in the orbit semi-major axis (Δa_{decay}) and orbital period (Δt_{decay}) of:

$$\begin{aligned}\Delta a_{decay} &= 2k\left|\delta a\right| \\ \Delta t_{decay} &= 2k\left|\delta\tau\right|\end{aligned} \tag{6}$$

Δt_{decay} is also the time between the necessary orbit correction manoeuvres. The correction manoeuvre can be computed with a Hohmann transfer:

$$\Delta V_{decay,\,i} = \sqrt{\frac{\mu_e}{r_1}}\left(\sqrt{\frac{2r_2}{r_1+r_2}}-1\right)+\sqrt{\frac{\mu_e}{r_2}}\left(1-\sqrt{\frac{2r_1}{r_1+r_2}}\right) \tag{7}$$

where μ_e is the gravitational parameter of the Earth, $r_1 = a_0 - \Delta a_{decay}$ is the radius of the initial circular orbit, and $r_2 = a_0$ is the radius of the final orbit after the manoeuvre. The total ΔV_{decay} due to the orbital height correction manoeuvres for the entire mission lifetime is the sum of the contribution of Eq. (7) every Δt_{decay} so that:

$$\Delta V_{decay} = \left\lfloor \frac{t_m}{\Delta t_{decay}} \right\rfloor \Delta V_{decay,\,i} \tag{8}$$

where $\left\lfloor t_m / \Delta t_{decay} \right\rfloor$ represents the number of manoeuvres to be executed during the mission lifetime t_m.

In addition, the orbit inclination needs to be controlled during the lifetime of a sun-synchronous spacecraft. The variation of the orbital inclination in fact causes the drifting of the line of the nodes and affects ground track repetition. The total ΔV_{inc} needed to compensate for the inclination variation can be computed as:

$$\Delta V_{inc} = 2\sin\left(\frac{\Delta i_{\text{sec}}}{2}\right)\cdot t_m \tag{9}$$

where Δi_{sec} is the secular variation of the inclination in one year that can be assumed equal to 0.05 deg/year, and t_m is the mission time in years.

To compute the ΔV_{inj} needed to compensate for injection errors, we assume that the maximum errors in the orbital parameters after launch are:

$$\begin{aligned} \Delta a_{inj} &= \pm 35\ km \\ \Delta i_{inj} &= \pm 0.2\ \text{deg} \end{aligned} \tag{10}$$

The ΔV_{inj} due to the injection errors can then be computed using a Hohmann transfer with plane change where the initial and final orbits have a radius of $r_1 = a_0 - \Delta a_{inj}$ and $r_2 = a_0$ respectively, and the inclination change is equal to Δi_{inj}.

Finally, the ΔV_{disp} to ensure the end-of-life disposal of the satellite can be computed as follows. Assuming that a 600 km altitude is the altitude from which the spacecraft will decay naturally within 25 years, it is possible to consider as a disposal manoeuvre, a Hohmann transfer from the nominal orbit to the 600 km orbit.

The sum of the previously computed delta-V values is the total ΔV_{tot} budget of a sun-synchronous mission, which depends on the nominal orbit of the spacecraft, the mission duration, and the characteristics of the spacecraft (mass, cross-section, drag coefficient).

$$\Delta V_{tot} = \Delta V_{decay} + \Delta V_{inc} + \Delta V_{inj} + \Delta V_{disp} \tag{11}$$

3.2 Tankage volume

For the purpose of this work, it is assumed that a monopropellant hydrazine propulsion system is adequate for all the orbit correction manoeuvres previously described. The specific impulse of hydrazine is 200 s. The propellant mass needed by the spacecraft during its entire lifetime can be computed using the Tsiolkowsky equation [30].

$$m_p = m_{s,\,in}\left(1 - e^{-\frac{\Delta V_{tot}}{g_0 Isp}}\right) \tag{12}$$

where m_p is the propellant mass needed to perform the total velocity change ΔV_{tot}, $m_{s,in}$ is the initial spacecraft mass, g_0 is the gravitational acceleration at sea level (equal to 9.81 m/s^2), and Isp is the specific impulse of the fuel used.

Once the propellant mass is calculated, the tankage volume can be estimated as

$$v_p = K1 \cdot \frac{m_p}{\rho_f} \tag{13}$$

where ρ_f is the density of hydrazine (equal to 1.02 g/cm^3), and $K1$ is a factor that takes into account the additional volume needed for the pressurant gas. For the entire article, $K1$ is assumed to have a value of 1.4 (average value from [32])

As an example, let us consider the MetOp mission [33]. MetOp is a sun-synchronous satellite with a mass of 4085 kg, and an average cross section S = 18 m^2. The operational orbit of the mission is 817 km in altitude with an inclination of 98.7 degrees. The mission design life is 5 years. Computing the mass of propellant with Eq. (12) returns a value of 360 kg of propellant, which is 12.5% more propellant than the actual mission of 320 kg. This is a reasonably close value considered considering the approximate delta-V budget procedure. Moreover, the value used for the specific impulse in the article (200 s) is lower than the actual characteristics of the MetOp mission thrusters, which ranges between 220 s and 230 s. Using these two values, the resulting propellant mass would range between 332 kg and 321 kg, a much closer value to the original mission.

As another example, Cryo-Sat2 [34] is a 3 years mission with a satellite mass of 720 kg, an average cross section of 8.8 m^2, and an orbital altitude of 717 km. The resulting propellant mass is 43 kg that is in good agreement with the value of 38 kg of the actual mission.

4 Multi-objective Optimisation

The demisability and survivability models have been implemented into a multi-objective optimisation framework. The purpose of this framework is to find preliminary, optimised spacecraft configurations, which take into account both the survivability and the

demisability requirements. In this way, a more integrated design can be achieved from the early stages of the mission design. The requirements arising from the demisability and the survivability are in general competing; consequently, optimised solutions represent trade-offs between the two requirements.

In its most general form, a multi-objective optimisation problem can be formulated as:

$$\begin{aligned} &\text{Min/Max } f_m(x), && m = 1,2,...,M; \\ &\text{Subject to } g_l(x) \le 0, && l = 1,2,...,\text{L} \\ &h_b(x) = 0, && b = 1,2,...\text{B}; \\ &x_i^{(L)} \le x_i \le x_i^{(U)}, && i = 1,2,...,n. \end{aligned} \tag{14}$$

where x is a solution vector, f_m is the set of the m objective functions used, g and h are the constraints and $x^{(l)}$ and $x^{(U)}$ are the lower and upper limits of the search space.

In multi-objective optimisation, no single optimal solution exists that can minimise or maximise all the objective functions at the same time. Therefore, the concept of Pareto optimality needs to be introduced. A Pareto optimal solution is a solution that cannot be improved in any of the objective functions without producing a degradation in at least one of the other objectives [35, 36].

There exists a large variety of optimisation strategies; however, for the purpose of this work and for the characteristics of the problem in question, genetic algorithms have been selected. The Python framework Distributed Evolutionary Algorithms in Python (DEAP) [37] was selected for the implementation of the presented multi-objective optimisation problem. Specifically, the selection strategy used is the Non-dominated Sorting Genetic Algorithm 2 (NSGAII) [36]. For the crossover mechanism, the Simulated Binary Bounded [38] operator was selected whereas for the mutation mechanism the Polynomial Bounded [39] operator was the choice.

Throughout this article, the input parameters to the genetic algorithm that define the characteristics of the evolution were fixed: the size of the population was set to 80 individuals, and the number of generations was set to 60. The crossover and mutation probability were 0.9 and 0.05 respectively.

4.1 Optimisation variables and constraints

The variables (vector x in Eq. (14)) of the optimisation process relate to the internal components, specifically the propellant tanks. The variables to be optimised were the tank material, the thickness, the shape, and the number of tanks. The total tankage volume, which in turn influences the internal radius of the tanks, is determined using Eq. (13) and depends on the mission scenario.

For the material, the possible options are limited to three different materials typically used in spacecraft tank manufacturing. The possible materials are aluminium alloy Al-6061-T6, titanium alloy Ti-6Al-4V, and stainless steel A316. The characteristics of these materials are summarised in Table 1.

Table 1: Properties of the materials used in the optimisation [40, 41].

	Al-6061-T6	A316	Ti-6Al-4V
ρ_{mat} (kg/m^3)	2713	8026.85	4437
T_m (K)	867	1644	1943
C_m (J/kg-K)	896	460.6	805.2
h_f (J/kg)	386116	286098	393559
ε	0.141	0.35	0.3
σ_y (MPa)	276	415	880
σ_u (MPa)	310	600	950
C (m/s)	5100	5790	4987

The shape of the tanks can take two different geometries: a spherical tank or a right cylindrical tank, (represented in the optimisation using a binary value). These geometries were chosen because they are typical of actual tank designs.

The number of tanks in which the propellant can be divided was varied from one to six units. It was assumed that six tanks would be a reasonable upper limit for the possible number of tanks to adopt.

Lastly, the thickness of the tanks can be varied in the range 0.5 mm to 5 mm. This was considered a reasonable range for actual spacecraft tanks. Values smaller than 0.5 mm are considered too small, and more suitable for tank liners. Values larger than 5 mm were excluded because very thick metallic tanks would be too heavy. A summary of the variables of the optimisation with their respective values and range is provided in Table 2

Table 2: Summary of optimisation variables.

Variable	Range/Values	Variable type
Tank material	Al-6061-T6, Ti-6Al-4V, A316	Integer
Tank number	1 to 6	Integer
Tank thickness	0.0005 to 0.005 m	Real
Tank shape	Sphere, Cylinder	Integer

4.2 Definition of fitness functions

The developed multi-objective optimisation framework uses the demisability and survivability models (see Section 2) to compute the fitness functions. These fitness functions allow the evaluation of a certain spacecraft configuration against the demisability and

survivability. In addition, they allow the comparison between different solutions, giving the optimiser the possibility to rank the different solutions according to their demisability and survivability.

To evaluate the level of demisability of a certain configuration, the Liquid Mass Fraction (LMF) is introduced. The LMF index represents the proportion of the total re-entering mass that melts during the atmospheric re-entry. In mathematical terms, the LMF index can be expressed as:

$$LMF = 1 - \frac{\sum_{j=1}^{N} m_{fin,j}}{\sum_{j=1}^{N} m_{in,j}} \tag{15}$$

where $m_{fin,j}$ and $m_{in,j}$ are the final and initial mass of the j-th component respectively, and N is the total number of components.

To evaluate the level of survivability, the probability of no-penetration (PNP) was selected as the survivability fitness function. The probability of no-penetration represents the chance that a specific spacecraft configuration is not penetrated by space debris during its mission lifetime. In this case, the penetration of a particle is assumed to produce enough damage to the components to seriously damage them so that the PNP can be considered a sufficient parameter to evaluate the survivability of a satellite configuration. The overall probability of no-penetration of a spacecraft configuration is given by:

$$PNP = 1 - \sum_{j=1}^{N} P_{p,\mathrm{j}} \tag{16}$$

where $P_{p,j}$ is the penetration probability of the j-th component.

4.3 Optimisation setup

As the demisability and the survivability are complex and require many different inputs, it is necessary to take into account all these different parameters. It is not only necessary to define the variables of the optimisation (see Section 4.1), but also all the other parameters needed by the two models to carry out their computations. One of the main aspects to define is the mission scenario (see Section 4.3.1) for both the demisability and the survivability. In the first case, this means taking a decision about the initial conditions of the atmospheric re-entry. In the second case, the operational orbit of the satellite and the mission duration need to be defined.

In the present work, the objective of the optimisation is to optimise tank configurations. Two aspects of the tank configuration that arw not directly taken into account by the optimisation variables is the size and sposition of the tanks (see Section 4.3.3). It was decided to relate the size of the tanks, i.e. the radius, to the total tankage volume (see Section 3.2) and to the number of tanks (see Eqs. (19) and (20)) in order to have a more realistic mission scenario. Delta-V budgets are in fact one of the main constraints on the mission design process and the amount of propellant, which is related to the size of the tanks, needs to be sufficient for the mission requirements. For what concerns the tank configurations, it was decided that, for the current stage of development of the project, the introduction of the optimisation of the positions of the tanks inside the spacecraft would have been too complex. For this reason, a predefined set of positions for the tanks was adopted (see Section 4.3.3).

Finally, both the demisability and the survivability analysis cannot be carried out without knowing the characteristics of the main spacecraft structure, i.e. the overall size and mass of the satellite, the material, the thickness and the type of shielding (see Section 4.3.2).

4.3.1 Mission scenarios

For the demisability simulation, the initial re-entry conditions are represented by the altitude, the flight path angle, the velocity, the longitude, the latitude, and the heading angle. Standard values for these parameters [22, 42] were selected and are presented in Table 3.

Table 3: Initial conditions for the re-entry simulations.

Parameter	Symbol	Value
Altitude	h_{in}	120 km
Flight path angle	γ_{in}	0 deg
Velocity	v_{in}	7.3 km/s
Longitude	λ_{in}	0 deg
Latitude	φ_{in}	0 deg
Heading	χ_{in}	-8 deg

For the survivability, the mission scenario is defined by the operational orbit of the satellite. As previously introduced (see Section 3), we are considering sun-synchronous missions. For this reason, the orbits selected need to satisfy the sun-synchronicity requirement. Specifically, orbits with an inclination of 98 degrees and an altitude of 800 km were chosen. In addition, four different mission durations were selected: 3, 5, 7, and 10 years.

4.3.2 Spacecraft configuration

The variables of the optimisation are related to internal components; however, the external configuration of the satellite still needs to be defined in order to perform the demisability and the survivability analysis. The first decision concerns the shape and the dimension of the outer structure of the satellite. It was decided to adopt a cubic shaped spacecraft in order to

keep the analysis as general as possible. The dimensions of the cubic structure (i.e. its side length) can be computed tacking into account the mass of the satellite (m_s) and assuming an average density for the satellite (ρ_s) as follows [30].

$$L = \sqrt[3]{m_s / \rho_s} \tag{17}$$

It was assumed that the density of the spacecraft is 100 kg/m^3, which is an average value that can be used in preliminary design computations [30].

Four classes of satellites were considered in the present analysis. The classes were defined according to the mass of the spacecraft: 500 kg, 1000 kg, 2000 kg, and 4000 kg options were considered. The classes and the corresponding spacecraft size, computed with Eq, (17) are summarised in Table 4.

Table 4: Mission classes analysed with respective size of the satellite.

Class	Side length
500 kg	1.7 m
1000 kg	2.15 m
2000 kg	2.7 m
4000 kg	3.4 m

In addition to the size and mass of the spacecraft, the thickness and material of the external wall also need to be defined. For the purpose of this work, and in order to maintain the same conditions for all the simulations, it was decided to use a single wall configuration with a 3 mm wall thickness made of Aluminium alloy 6061-T6.

4.3.3 Tank configurations

To describe the possible tank configurations, a series of assumptions were made in order to limit the complexity of the problem so that it could be analysed within the current capabilities of the demisability and survivability models developed (Section 2). The first assumption was to limit the maximum number of tanks to six units (i.e. the total propellant mass cannot be divided into more than six tanks). The second assumption concerns the disposition of the tanks inside the spacecraft. Because of the limitations on the position of the centre of mass of the satellite, it was decided to equally space the tanks around the centre of mass. The centre of each tank is placed at the vertices of a regular polygon and the barycentre of the polygon coincides with the centre of the main spacecraft structure. For example, three tanks would be positioned as an equilateral triangle, four tanks as a square, and so on. As the tanks obviously cannot intersect each other, their mutual distance has to be bigger than twice their radius. With this consideration, the side length of the polygons can be computed as:

$$l = 2r_t \cdot K2 \tag{18}$$

where r_t is the tank radius, and $K2$ is a multiplicative factor to take into account the spacing between two tanks. For the analysis presented in this paper, $K2$ has a value of 1.2.

As the total tankage volume is fixed by the mission characteristics and computed through Eq. (13), the external radius of the tank can be related to the number of tanks in the configuration as follows. For spherical tanks, we have:

$$r_t = \sqrt[3]{\frac{3}{4\pi} \cdot \frac{v_p}{n_t}} + s_t \tag{19}$$

Whereas for right cylindrical tanks

$$r_t = \sqrt[3]{\frac{1}{2\pi} \cdot \frac{v_p}{n_t}} + s_t \tag{20}$$

where r_t is the outer radius of the tank, n_t is the number of tanks in the configuration, and s_t is the thickness of the tank. An example of a configuration with four tanks is presented in Figure 1.

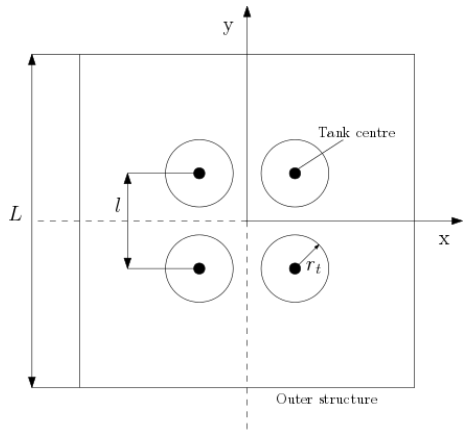

Figure 1: Example of a tank configuration with four tanks equally spaced with respect to the centre of mass of the spacecraft.

5 Results and Discussion

This section presents the results obtained through the multi-objective optimisation framework previously described (see Section 4). The results were used to analyse the influence of the spacecraft design and of the mission characteristics on the demisability and the survivability when these factors are considered in combination. The influence of the mission characteristics in term of the mass of the spacecraft (see Table 4) and the mission lifetime were taken into account. The effect of the tank configuration with respect to the tank material, size, thickness, shape and number of vessels was also considered.

The analysis considered cylindrical and spherical tanks with varying thickness, material, and number of vessels. The possible tank configurations ranged from one to six tanks and were arranged in a simplified fashion shown in Figure 2. The circles represent the positions of the centre of each tank. The size and positioning of the tanks follows the procedure of Section 4.3.3. In each configuration, the tanks have the same shape, i.e. they are all spheres or cylinders.

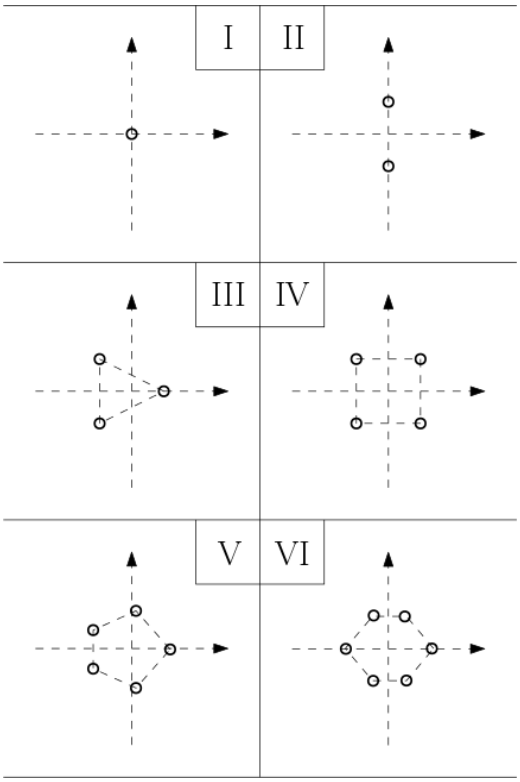

Figure 2: Possible configuration for the positioning of the spacecraft tanks.

Different optimisation simulations were performed varying the range of the number of tanks, i.e. not just performing the simulations with the maximum possible number of tanks.

An example of the Pareto front obtained with the optimisation is shown in Figure 3. The presented Pareto front was obtained for a 2000 kg spacecraft in an 800 km altitude orbit, with a maximum number of tanks allowed equal to three (configurations I, II, and III of Figure 2. Probability of No-Penetration, and the y-axis represents the demisability index, i.e. the Liquid Mass Fraction. Both indices are expressed in terms of percentage. It is possible to observe the general trend of the Pareto front, with the aluminium solutions in the upper part (blue solutions), representing the solutions with higher demisability but also a higher vulnerability to debris impacts. The stainless steel solutions (orange solutions) are instead on the right part of the graph, corresponding to solutions with higher survivability but lower demisability. No titanium solutions are present. This is a common result for all the simulations performed, due to the extremely low demisability of titanium and its impact resistance comparable to stainless steel.

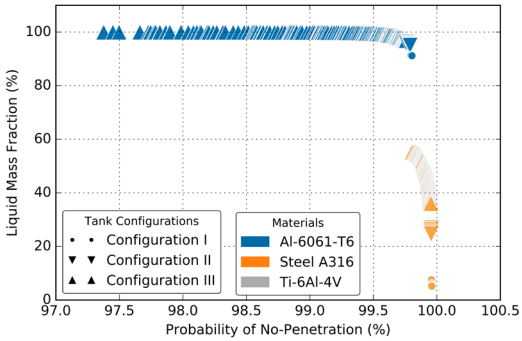

Figure 3: Pareto front for a 2000 kg spacecraft and 10-year mission with a maximum allowed number of tanks equal to three.

The x-axis represents the survivability index, i.e. the

A gap is also observable between the aluminium and the stainless steel solutions. This is caused by the considerable difference between the demisability of the two materials. In fact, two solutions with a slightly different survivability coming from the different combination of material and thickness can have a remarkable difference in the demisability because of the high influence of material properties on the demisability. All the solutions obtained by the optimiser represent configurations with cylindrical tanks. In general, no solutions with spherical tanks were obtained for the conditions used in this study.

Another interesting consideration is the influence of the number of tanks in the configuration. As it is possible to observe, in this case, all three configurations are viable solutions after the optimisation. Configurations with lower amount of tanks have higher survivability and the lower demisability. This is because the smaller the number of tanks in which to split the propellant, the bigger the tanks are and thus the less demisable they are. However, they also have a lower external surface, which in turn means a higher survivability. On the other hand, configurations with a higher number of tanks have smaller and more demisable tanks but a higher external surface. They are also positioned closer to the external walls making them more vulnerable to the debris impacts.

Figure 4 and Figure 5 represent two further examples of Pareto fronts for the previously introduced mission scenario. In these cases, the maximum allowed number of tanks was respectively four and six. As it is

possible to observe in Figure 4 the only solutions resulting from the optimisation are those corresponding to Configuration IV, with four tanks. Figure 5 has more variety of solutions with configurations comprising four, five and six tanks. However, there is a clear predominance of solutions with six tanks. In general, in all the optimisations performed, for the different classes and mission scenarios, this trend was repeated.

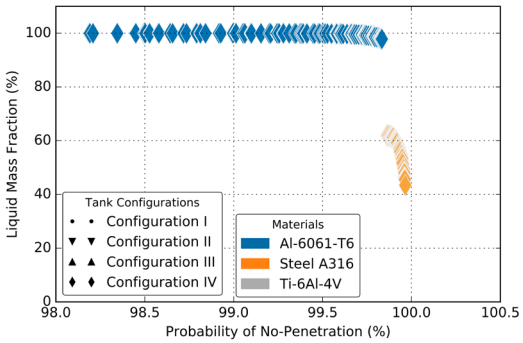

Figure 4: Pareto front for a 2000 kg spacecraft and 10-year mission with a maximum allowed number of tanks equal to four.

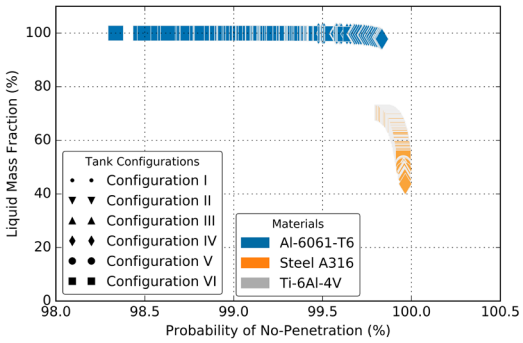

Figure 5: Pareto front for a 2000 kg spacecraft and 10-year mission with a maximum allowed number of tanks equal to six.

The majority of the solutions were represented by the maximum allowed number of tanks. Despite the fact that a higher number of tanks is also more exposed to debris impact, it is possible for the optimiser to find solutions with a higher thickness to compensate for this while still maintaining a higher demisability than a solution with a lower number of tanks. When this is no longer the case within the specified ranges of the optimisation, solutions with a lower number of tanks become better. This behaviour is strictly correlated with how the demisability index is defined (see Eq. (15) where the proportion of mass demised is considered. This is a reasonable choice for a demisability index. In fact, while it is true that even a partially melted object reaches the ground and contributes to the casualty risk, the uncertainty in re-entry simulations [43, 44] make the LMF index a good indication of how likely the considered object will demise. It is in fact important to remember that the presented methodology involves a preliminary assessment of many configurations. A further, more refined, analysis of the most promising configurations can then be carried out to verify their quality. Another observable trend within Figure 3, Figure 4, and Figure 5 is the reduction of the demisability gap between the aluminium alloy and the stainless steel solutions. As the number of tanks increases, the maximum demisability of the stainless steel solutions also increases, closing the gap with the aluminium alloy solutions. This indicates that to have demisable solutions for tanks made of stainless steel, it is necessary to increase the number of vessels used, as only smaller tanks will be demisable.

As introduced in the previous paragraphs, the mission characteristics have also been taken into account. In particular, the size of the spacecraft in terms of mass and external dimension (see Table 4), and the mission lifetime. These aspects influenced the optimisation results, changing the shape and the features of the Pareto fronts. For example, the minimum value of the PNP index corresponds to the configuration with the best demisability but also the worst survivability. Such information gives an idea of how much an improved demisability can compromise the survivability of a spacecraft, and as a function of the mission scenario. In Figure 6, it is possible to observe the variation of the minimum survivability for each optimisation simulation as a function of the mission class and lifetime, and for four different tank configurations.

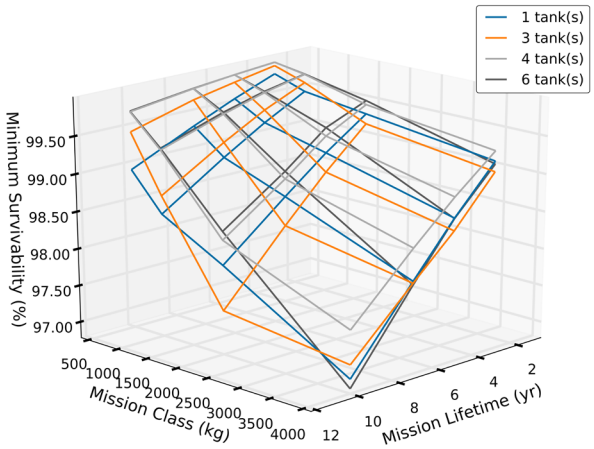

Figure 6: Minimum survivability of the solutions in the Pareto front as a function of the mission class and lifetime.

As expected, the higher the mission lifetime, the lower the value of the minimum survivability. The same happens as we increase the mission class. In fact, bigger

spacecraft have a bigger probability of being hit by space debris. The figure shows that for smaller spacecraft with limited lifetimes an enhanced demisability may not compromise their survivability, giving the design team the possibility to push to more extreme solutions favouring the demise. On the other hand, more massive and longer mission may need a more refined study because very demisable solutions may compromise the reliability of the mission with respect to debris impacts. The difference is in fact in the order of 2.5%, which is not negligible. In fact, the penetration probability of complete spacecraft configurations is usually in the order of few percentage points (1-5%) [28]. Therefore, having the survivability of just one component hampered by 1% or 2% would have a big relative impact on the overall survivability of a spacecraft. It is true that this is a simplified simulation and many things can be changed in a spacecraft configuration to make it less vulnerable, for instance the outer shielding. However, this study gives a first order evaluation of what the effects can be when the survivability and the demisability are considered at the same time.

Another feature of the Pareto front that is heavily influenced by the simulation class and mission duration is the demisability gap that is present between the aluminium solution with the smallest demisability and the steel solution with the highest demisability. This gap provides an indication of how difficult it is for steel solutions to reach a comparable demisability level with respect to aluminium solutions. Figure 7 shows a representation of the trend relating to this demisability gap. As it is possible to observe, the higher the number of tanks in the configuration, the smaller the gap for every type of mission scenario.

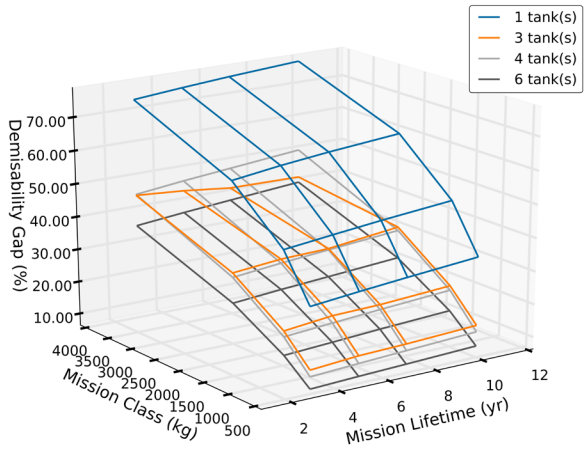

Figure 7: Demisability gap between the solutions in the Pareto front as a function of the mission class and lifetime.

There is a considerable gap between the solution with one tank and the other solutions with multiple tanks. It is also possible to observe that the configurations with three and four tanks are very close and produce similar results. It is also evident that the mission size is much more influential than the mission lifetime for this specific characteristic. Bigger missions have larger tanks, which are of course more difficult to demise. This has a bigger impact on solutions with less demisable materials such as the stainless steel.

5.1 Optimisation indices discussion

The optimisation framework presented in the previous paragraphs was aimed at demonstrating the interdependence of the demisability and the survivability requirements when it comes to the design of spacecraft components and configurations. To do so, a simplified spacecraft design with a single type of internal component (i.e. tanks) was selected. In order to relate the results obtained to actual mission scenarios, the propellant mass and, as a consequence, the dimensions of the tanks was related to the delta-V budget of sun-synchronous missions (see Section 3). The optimiser was left free to look for solutions inside the search space defined in Table 2. No other constraints were added to the optimisation problem. For example, there was no limit on the overall mass of the configuration or complexity of the propulsion regulation system, and no check if the tanks were sufficiently strong to withstand the common storage pressures, etc.

It is thus interesting to compare the obtained solutions against some of these characteristics. In Figure 8 a Pareto front is presented for a 2000 kg class mission with seven years of mission lifetime and a maximum allowed numbers of tanks equal to three.

To the plot is associated the variation of the ratio between the tank configuration mass and the propellant mass for each solution. As it is possible to observe, the mass tends to increase as the solutions move from the more vulnerable and more demisable solutions to the more survivable and less demisable solutions. However, there are solutions corresponding to configurations with a number of tanks lower than the maximum allowed, which have a lower mass thus producing the valleys in the graph.

Usually spacecraft propellant tanks have a mass raging between 10% and 20% of the propellant mass stored, and they can reach 50% for high storage pressures [30]. In Figure 8, such solutions are highlighted in red in both plots. It is possible to observe that only aluminium alloy solutions belong to the typical mass range for the specific mission. However, some stainless steel solutions are not too far away from the considered range and, considering this is a preliminary design analysis, some of them could be included during

the later stages of the mission design process. In addition, it is possible to observe that all three kinds of configuration (one, two and three tanks) are present in the typical range, giving a wider variety of options to the design team.

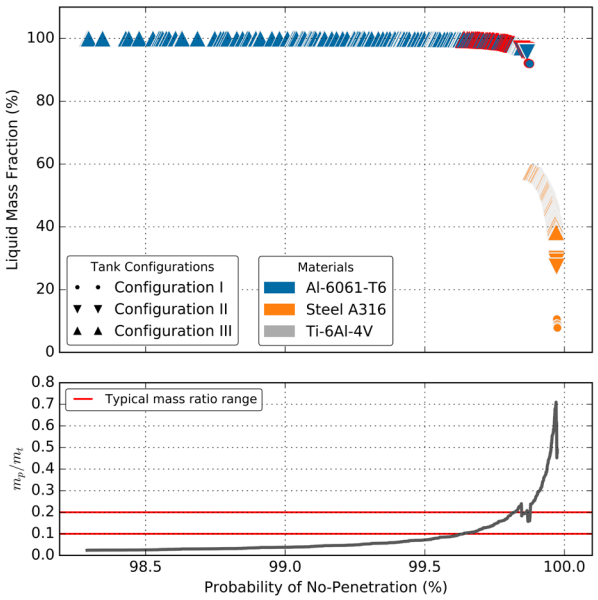

Figure 8: Pareto front for a 2000 kg, 7 years mission with maximum 3 tanks, with variation of the ratio between the tank configuration and the propellant mass. Highlighted (red lines and symbols) the solutions inside the typical range for actual missions.

Another important aspect to look at is the actual feasibility of the solutions, i.e. whether the tanks are actually able to sustain the normal operating pressures. Typically, a propellant tank has a storage pressure between 2 and 4 MPa. For cylindrical tanks, which constitute the solutions obtained in the Pareto front, the stress on the tanks' walls can be computed as follows:

$$\sigma_w = \frac{p r_t}{s_t} \tag{21}$$

where σ_w is the stress on the walls of the tank, and p is the storage pressure.

The computed tension has to be lower than the ultimate tensile strength of the material of the tank. This in turn imposes a limit on the maximum pressure that a tank with a certain radius, thickness and material can withstand, which is [30]:

$$p_{\max} = \frac{\sigma_u \cdot s_t}{r_t \cdot SF} \tag{22}$$

where σ_u is the ultimate tensile strength of the material, and SF is a safety factor assumed equal to 1.5 for the current study.

In Figure 9 the same Pareto front as before is presented. In this case the second plot represent the maximum sustainable storage pressure of the solutions belonging to the Pareto front and computed with Eq. (22). Even in this case, the solutions within the common limits (2-4 MPa) have been highlighted in red. As it is possible to observe, both aluminium alloy and stainless steel solutions belong to the highlighted range. Obviously, all the stainless steel solutions would be viable as they can resist a storage pressure higher than the 4 MPa limit. The aluminium alloy solutions outside the range, on the other hand, would be too thin to withstand the operating pressures normally used.

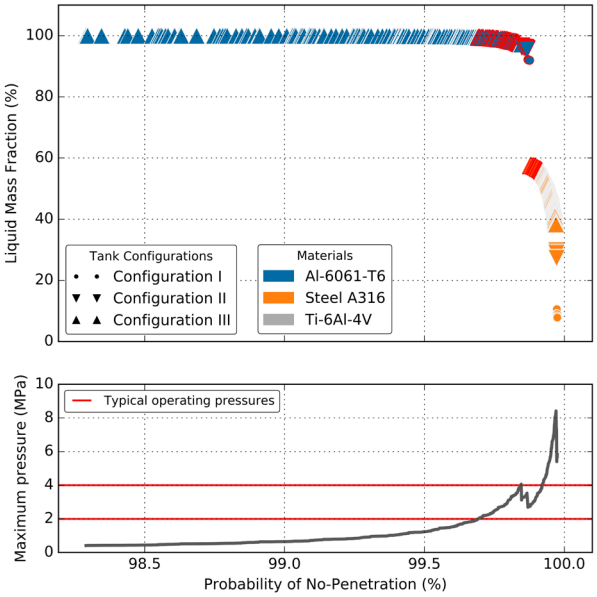

Figure 9: Pareto front for a 2000 kg, 7 years mission with maximum 3 tanks, with variation of the maximum storage pressure. Highlighted (red lines and symbols) the solutions inside the typical range of propellant storage pressures.

Finally, we can consider a more casualty risk related parameter that is the on-ground impact energy. As was mentioned, the demisability index adopted in this study has some limitations because it only considers the percentage of demised mass. However, it is also important to know the mass that actually lands on the surface, and even more important is to know the impact energy of the re-entering object. In fact, the NASA standard [3] states that a surviving object does not pose a risk for people on the ground if it has an impact energy below 15 J. This means the impact energy is an important parameter when considering the demisability of spacecraft components. In Figure 10, the impact energy of each solution in the Pareto front is represented. There are many solutions below the 15-joule threshold; however, all of them are made of aluminium alloy. Stainless steel solutions reaching the

surface are usually too heavy to have such a low impact energy. However, the 15-joule limit is quite specific and, given the uncertainty intrinsic to re-entry simulations, it probably should not constitute a hard boundary to the validity of a solution, especially during a preliminary design phase.

It is evident from this analysis of the solutions obtained from the optimisation that some improvements need to be introduced to the formulation of the optimisation itself. In fact, it is more efficient and more useful to obtain solutions that already take into account mission related constraints such as the overall mass of the system or its strength, as well as the casualty risk requirements. This can be obtained through a different definition of the fitness functions. For example, by changing the demisability index so that it includes a way to take into account the impact energy of the re-entering components. Moreover, a set of constraints can be introduced during the optimisation to take into account the limitations such as the maximum allowed storage pressure.

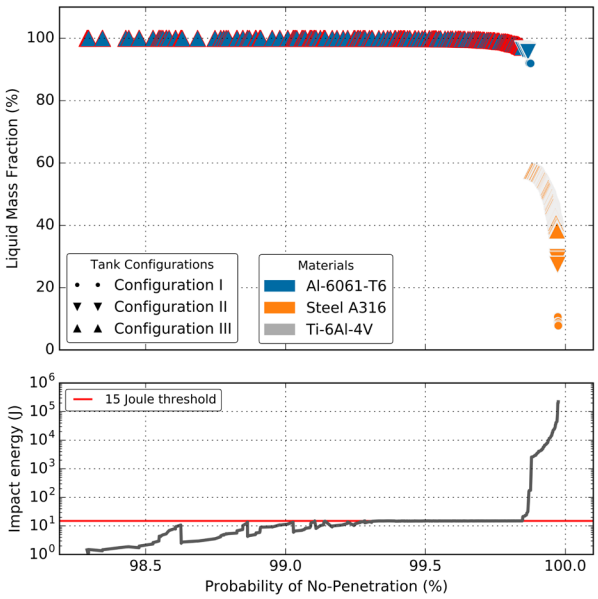

Figure 10: Pareto front for a 2000 kg, 7 years mission with maximum 3 tanks, with variation of the final energy of the re-entering object. Highlighted (red lines and symbols) the solutions below the 15 J threshold.

6 Conclusions

An optimisation framework that analyses preliminary spacecraft design options against the requirements posed by the demisability and the survivability was proposed. This optimisation framework has been applied to sun-synchronous missions and to a specific type of component, i.e. tanks, in order to study its behaviour and the influence of such requirements on the design choices. Two fitness functions describing the demisability and the survivability have been presented, and different tank configurations have been analysed as a function of their material, geometry and configuration. The optimiser is able to provide a wide range of solutions for different types of mission scenarios. Some trends could be observed in the output of the optimisation for the different scenarios as a function of the mission class, lifetime and of the maximum allowed number of tanks in the configuration. For example, no titanium solutions were observed, nor were configurations with spherical tanks obtained.

A more in depth analysis of the solutions obtained showed that only a subset of the solutions belonged to typical configurations with respect to the mass and strength of the configuration. Moreover, only certain solutions in the Pareto front could satisfy the casualty risk criterion of the 15-joule threshold. This means that a further effort needs to be made in the definition of the optimisation problem through a more tailored definition of the demisability and survivability indices and through the application of constraints during the optimisation. Considering these additional properties may lead to a different set of solutions. For example, spherical tanks may be present because of their capability to withstand higher storage pressures with respect to cylindrical tanks with the same volume.

Acknowledgments

Part of this work was funded by EPSRC DTP/CDT through the grant EP/K503150/1.

Thanks also to the European Space Agency for sponsoring the attendance to the 2016 IAC under the International Space Education Board participation programme.

References

[1] B. O'Connor 2008. Handbook for Limiting Orbital Debris. NASA Handbook 8719.14. *National Aeronautics and Space Administration, Washington, DC*.

[2] F. Schäfer, M. Lambert, E. Christiansen *et al.* The inter-agency space debris coordination committee (IADC) protection manual. 4th European Conference on Space Debris, 2005.

[3] NASA 2012. Process for Limiting Orbital Debris. Washington, DC USA.

[4] ESA 2008. Requirements on Space Debris Mitigation for ESA Projects.

[5] R. L. Kelley 2012. Using the Design for Demise Philosophy to Reduce Casualty Risk Due to Reentering Spacecraft.

[6] P. M. Waswa, and J. A. Hoffman 2012. Illustrative NASA Low Earth Orbit spacecraft

subsystems design-for-demise trade-offs, analyses and limitations. *International Journal of Design Engineering,* 5**,** 21-40.

[7] P. M. B. Waswa, M. Elliot, and J. A. Hoffman 2013. Spacecraft Design-for-Demise implementation strategy & decision-making methodology for low earth orbit missions. *Advances in Space Research,* 51**,** 1627-1637.

[8] E. Christiansen 2009. Handbook for Designing MMOD Protection. Huston, Texas USA.

[9] R. Putzar, and F. Schäfer, *Vulnerability of spacecraft equipment to space debris and meteoroids impacts,* Final Report, vol. 1, European Space Agency, 2006.

[10] L. Grassi, F. Tiboldo, R. Destefanis *et al.* 2014. Satellite vulnerability to space debris – an improved 3D risk assessment methodology. *Acta Astronautica,* 99**,** 283-291.

[11] M. Trisolini, H. G. Lewis, and C. Colombo. Survivability and Demise Criteria for Sustainable Spacecraft Design. 66th International Astronautical Conference, 2015 Jerusalem.

[12] H. Schaub, L. E. Jasper, P. V. Anderson *et al.* 2015. Cost and risk assessment for spacecraft operation decisions caused by the space debris environment. *Acta Astronautica,* 113**,** 66-79.

[13] M. Trisolini, H. G. Lewis, and C. Colombo, "Demise and Survivability Criteria for Spacecraft Design Optimisation," in International Association for the Avancement of Space Safety Conference, Melbourne, Florida, 2016.

[14] NASA. 2009. *ORSAT* [Online]. NASA Orbital Debris Program Office. Available: http://orbitaldebris.jsc.nasa.gov/reentry/orsat.html [Accessed July 14 2015].

[15] NASA. 2015. *Debris Assessment Software* [Online]. NASA Orbital Debris Program Office. Available: http://orbitaldebris.jsc.nasa.gov/mitigate/das.html [Accessed July 14 2015].

[16] T. Lips, and B. Fritsche 2005. A comparison of commonly used re-entry analysis tools. *Acta Astronautica,* 57**,** 312-323.

[17] E. Minisci 2015. Space Debris and Asteroids (Re)Entry Analysis Methods and Tools. Glasgow, UK: University of Strathclyde.

[18] R. D. Klett, *Drag Coefficients and Heating Ratios for Right Circular Cylinder in Free-Molecular and Continuum Flow from Mach 10 to 30,* Technical Report SC-RR-64-2141, Sandia Report, SC-RR-64-2141, Albuquerque, 1964.

[19] W. P. Hallman, and D. M. Moody, *Trajectory Reconstruction and Heating Analysis of Columbia Composite Debris Pieces*, The Aerospace Corporation, 2005.

[20] T. M. Owens. 2014. *Aero-Thermal Demise of Reentry Debris: A Computational Model.* Master of Science, Florida Insititute of Technology.

[21] J. Beck. May 5 2015. *RE: Personal Communication.*

[22] J. Beck, J. Merrifield, I. Holbrough *et al.* 2015. Application of the SAM Destructive Re-Entry Code to the Spacecraft Demise Integration Test Cases. 8th European Symposium on Aerothermodynamics of Space Vehicles, March 2015 2015 Lisbon.

[23] T. Lips, V. Wartemann, G. Koppenwallner *et al.* Comparison of ORSAT and SCARAB Reentry Survival Results. 4th European Conference on Space Debris, 18-20 April 2005 Darmstadt, Germany. 533.

[24] NASA 1976. U.S. Standard Atmosphere 1976. Washington, D.C.

[25] A. Tewari 2007. *Atmospheric and Space Flight Dynamics: Modeling and Simulation with MATLAB® and Simulink®*, Birkhäuser.

[26] S. Flegel 2011. MASTER-2009 Software User Manual. Institute of Aerospace Systems (ILR).

[27] N. Welty, M. Rudolph, F. Schäfer *et al.* 2013. Computational methodology to predict satellite system-level effects from impacts of untrackable space debris. *Acta Astronautica,* 88**,** 35-43.

[28] K. Bunte, R. Destefanis, and G. Drolshagen. Spacecraft Shielding Layout and Optimisation Using ESABASE2/Debris. Proc. 5th European Conference on Space Debris, 2009.

[29] A. Gäde, and A. Miller 2013. ESABASE2/Debris Release 6.0 Technical Description European Space Agency.

[30] J. R. Wertz, and W. J. Larson 1999. *Space Mission Analysis and Design*, Springer Netherlands.

[31] S. Platnick. 2016. *NASA's Earth Observing System* [Online]. National Aeronautics and Space Administration. Available: http://eospso.nasa.gov/mission-category/3 [Accessed January 2016].

[32] Airbus Safran Launchers GmbH. 2003. *Space Propulsion* [Online]. Bremen, Germany. Available: http://www.space-propulsion.com/index.html [Accessed July 2016].

[33] European Space Agency. 2012. *Metop - meteorological missions* [Online]. European Space Agency. Available: http://www.esa.int/Our_Activities/Observing_the_Earth/The_Living_Planet_Programme/Met

eorological_missions/MetOp/Overview14 [Accessed January 2016].

[34] European Space Agency. 2016. *CryoSat-2 (Earth Explorer Opportunity Mission-2)* [Online]. eoPortal Directory. Available: https://eoportal.org/web/eoportal/satellite-missions/c-missions/cryosat-2 [Accessed July 2016].

[35] K. Deb 2001. *Multi-objective optimization using evolutionary algorithms*, John Wiley & Sons.

[36] K. Deb, A. Pratap, S. Agarwal *et al.* 2002. A fast and elitist multiobjective genetic algorithm: NSGA-II. *Evolutionary Computation, IEEE Transactions on,* 6**,** 182-197.

[37] F. A. Fortin, F. M. De Rainville, M. A. Gardner *et al.* 2012. DEAP: Evolutionary Algorithms Made Easy. *Journal of Machine Learning Research,* 13**,** 2171-2175.

[38] K. Deb, and R. B. Agrawal 1995. Simulated binary crossover for continuous search space. *Complex systems,* 9**,** 115-148.

[39] K. Deb, and D. Deb 2014. Analysing mutation schemes for real-parameter genetic algorithms. *International Journal of Artificial Intelligence and Soft Computing,* 4**,** 1-28.

[40] J. N. Opiela, E. Hillary, D. O. Whitlock *et al.*, *Debris Assessment Software Version 2.0 - User's Guide*, Lyndon B. Johnson Space Center, Huston, Texas, 2012.

[41] ASM Aerospace Specification Metals Inc. 2016. *ASM Aerospace Specification Metals* [Online]. Pompano Beach, Florida. Available: http://www.aerospacemetals.com/contact-aerospace-metals.html [Accessed July 2016].

[42] B. Fritsche, T. Lips, and G. Koppenwallner 2007. Analytical and numerical re-entry analysis of simple-shaped objects. *Acta Astronautica,* 60**,** 737-751.

[43] J. Merrifield, J. Beck, G. Markelov *et al.* Aerothermal Heating Methodology in the Spacecraft Aerothermal Model (SAM). 7th IAASS Conference, 2014.

[44] J. Merrifield, J. Beck, G. Markelov *et al.* Simplified Aerothermal Models for Destructive Entry Analysis. 8th European Symposium and Aerothermodynamics for Space Vehicles, 2015.